



Contents lists available at ScienceDirect

Journal of King Saud University – Science

journal homepage: www.sciencedirect.com

Original article

Mechanism of interaction and removal of zinc with lignocellulosic adsorbents, closing the cycle with a soil conditioner



Birol Kayranli

Graduate School of Natural and Applied Science, Department of Environmental Science Gazi University, Ankara, Turkey

ARTICLE INFO

Article history:

Received 1 July 2021

Revised 7 August 2021

Accepted 9 September 2021

Available online 20 September 2021

Keywords:

Zinc removal
Lignocellulosic adsorbent
Removal mechanisms
Soil conditioner

ABSTRACT

Batch experiments were performed to remove Zn^{2+} by adsorption process using organic residuals (pistachio, peanut, and almond) as an adsorbent. The adsorbents were characterized by FTIR spectra, SEM images, and elemental analysis. Optimum adsorption of Zn^{2+} was obtained at pH 6 with a contact time of 45 min at room temperature with 1.0 g adsorbents. The adsorption of Zn^{2+} was found to well describe Langmuir isotherm model and a pseudo-second-order rate equation. The maximum adsorption capacity of pistachio, peanut, and almond is as follows; 59.52 mgg⁻¹, 54.64 mgg⁻¹, and 51.81 mgg⁻¹, respectively. Functional groups on shell surfaces can cooperate with metal ions in many ways such as electrostatic interaction, ion exchange, complex formation, and diffusion. This study has shown that pistachio, peanut, and almond shell can be used for reducing Zn^{2+} from aqueous solutions as an eco-friendly, low-cost adsorbent. The end-product containing organic compounds and zinc can be used as a soil conditioner. Furthermore, the usage of the organic shell as a sorbent for the capturing of zinc from contaminated water ensures both the technical advantage and cost-effectiveness for the sustainable environmental management concept.

© 2021 The Author(s). Published by Elsevier B.V. on behalf of King Saud University. This is an open access article under the CC BY-NC-ND license (<http://creativecommons.org/licenses/by-nc-nd/4.0/>).

1. Introduction

The production of zinc over the world was 10.5 Mt in 2019 with help of roasting, electrolysis and pyrometallurgical process, purifying and electrodeposition. Zinc is one of the metals mostly utilized in industrial, and agricultural processes, medicine, electroplating, mining, smelting, battery, paints and pigments, and pesticides due to its strong binding ability (Wang et al., 2020). However, zinc substances can be particularly toxic, and these elements are available from a wide variety of food sources. Zinc and its compound exposure exceed the permissible levels cause various health issues such as lung, bladder, breast, respiratory systems cancer, immune systems, gastrointestinal distress, and neurological signs (Ali et al., 2005; Neris et al., 2019a). Therefore, the allowable level of 5.0 mg/L in drinking water is released by the Environmental Protection Agency (EPA) and the World Health Organization (WHO).

E-mail addresses: bkayranli@gazi.edu.tr

Peer review under responsibility of King Saud University.



Zinc, a transition metal, is an essential micronutrient as well as metal, and the body and human immune systems need zinc to function properly. Zinc is also an essential cofactor required for the performing of biological processes in all life and helps in the growth of cells (Lonergan and Skaar, 2019). The lack of zinc deficiency brings about the loss of crops and retarded growth of plants. Moreover, the presence of organic materials affects nutrient ability and mobility, soil humidity and microorganism activity. So, the increase in soil organic contents results in an increase in soil water holding capacity, microorganism activity, nutrients, and mineral availability.

Some conventional process has been widely used for the reduction of heavy metals from aquatic solution, for instance, ion exchange, chemical precipitation, electrolysis, adsorption, electrocoagulant, membrane technologies (Ali et al., 2018b; Basheer, 2018; Mu'azu et al., 2019). However, most of these methods application has some limitation due to low efficiency and high operation costs. Among these, on the other hand, adsorption is called inexpensive, flexible, easy to operate in comparison to other processes, and a highly effective method for the reduction of metal from polluted water (Ali et al., 2018a; Hamad, 2021). However, researchers focus only on the adsorbent capacity and removal efficiency, rather than a comprehensive environmental protection approach to both metal removal and produced end-products (Ali et al., 2021b; Ali et al., 2021a).

<https://doi.org/10.1016/j.jksus.2021.101607>

1018-3647/© 2021 The Author(s). Published by Elsevier B.V. on behalf of King Saud University.

This is an open access article under the CC BY-NC-ND license (<http://creativecommons.org/licenses/by-nc-nd/4.0/>).

Peanut, pistachio, and almond are cultivated in the Middle East, the United States, and Mediterranean countries. Their annual production amount was about 47.0 million tons for peanuts, about 1.4 million tons for Pistachio, and about 3.2 million tons for almonds in 2019 (FAO, 2020). The shell indicates about 35–40% of the total dry weight of peanut and 50 % of pistachio, almond. and annually shell produce is 16–19, 0.7, and 1.6 million tons respectively. Millions of tons of different agricultural wastes are burned or commonly discharged and disposed of at landfills resulted in odour and favouring microbial growth (Oliveira et al., 2013). The presence of lignin, cellulose, and hemicellulose in pistachio, peanut, and almond shells make a valuable adsorbent for the purification of contaminated water by zinc and further beneficial usage of final products. Therefore, efficient researches are needed to find out a new adsorbent, recycle waste, is low-cost, obtaining end-products, and have a high adsorption capacity of heavy metals. When zinc wastes are removed by organic residuals and recovery properly, it could be used beneficially for agriculture with zinc enriched organic soil conditioner.

Therefore, the research aim is to assess the possible removal mechanism, adsorption capacity, and obtaining by-products in the removal of zinc ions from aqueous solutions, and also possible usage of end-product as a soil conditioner. Some kinetic and isotherm were used to analyse the adsorption process. The possible removal mechanism of the metals is also explained with the help of FTIR spectra and SEM images. The effects of time, Zn^{2+} concentrations, pH on metal removal efficiency were evaluated in batch experiments.

2. Materials and methods

2.1. Materials and chemicals

Local dried nut manufactory provided pistachio, peanut, and almonds shells. Previous to the ground and sieved, all shells were cleaned with deionized water and then dried out in the oven

(Memmert Universal UN750, Germany) at 105 °C for >24 h. The particle size of 0.5–1.2 mm was used as the adsorbents for further studies.

The chemicals, $ZnCl_2$ (96% purity), HCl, and NH_4OH , are of analytical grade and were provided from Merck Chemistry, Turkey. Deionized water (resistivity = $18.2 M\Omega cm^{-1}$) was produced from a Merck KGaA, Darmstadt, Millipore, Sigma system and used throughout the further study. Zn stock solution (1000 mg/L) was prepared with the help of exactly 2.09 g $ZnCl_2$ dissolved into 1 L pure water and the desired concentration of Zn^{2+} was diluted for the study. The value of pH measured using a pH 510 Eutech pH-meter in solution (100 mg/L) was adjusted to 6 by using 0.1 mol/L HCl or 0.1 mol/L NH_4OH .

2.2. FTIR measurements

The surface chemistry was studied with the help of FTIR spectroscopy. FTIR spectra were recorded using a Perkin Elmer 400 FTIR/FT-FIR) with a spectral resolution of $4 cm^{-1}$. FTIR spectra for three adsorbents is demonstrated in Fig. 1

2.3. SEM analyses

Scanning electron microscopy using a Zeiss Gemini 500–71–08 was used for the surface properties of the shell samples. The Origin® software was used to smooth the data. SEM images (magnification of 20,000) of the almond, peanut, and pistachio shells were taken with raw, and 10-minute intervals during removal of Zn^{2+} . SEM images is presented in (Fig. 2).

2.4. Analytical methods

Perkin Elmer Optima 2100 DV model inductively coupled plasma optical emission spectrometry (ICP-OES) was used to calculate the final Zn^{2+} concentrations after the designated contact time.

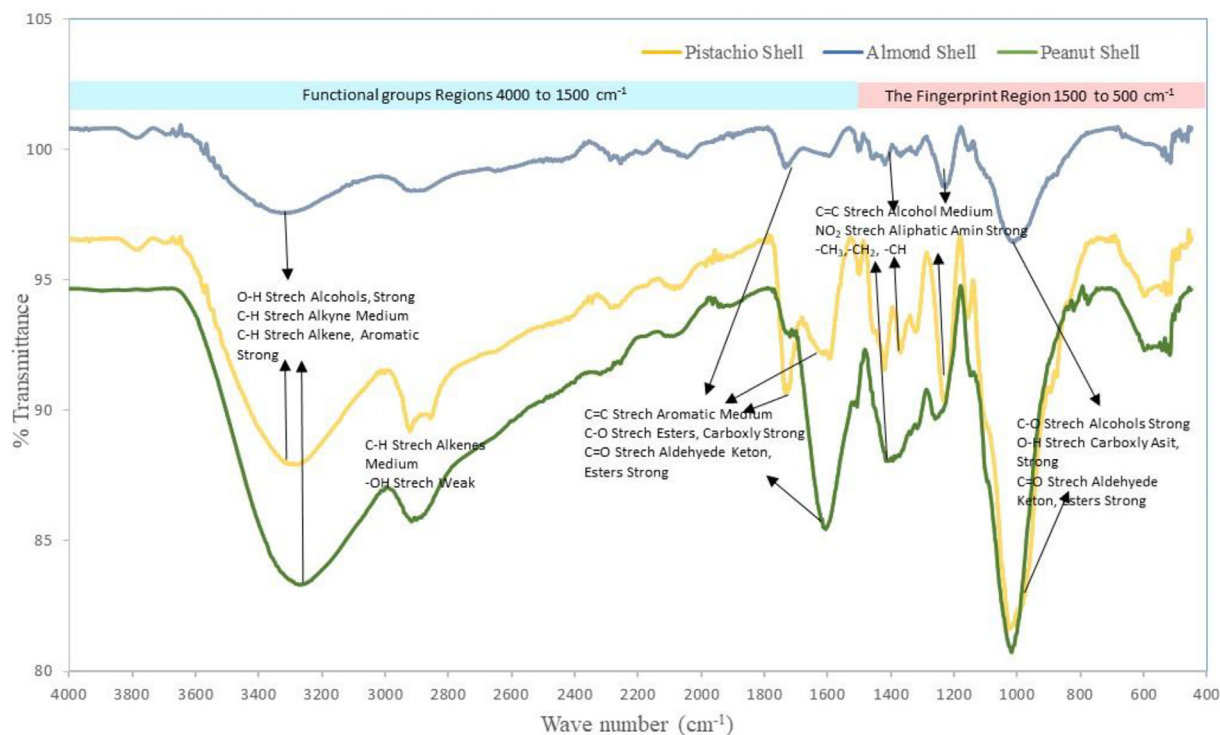


Fig. 1. Three adsorbent FTIR spectra and functional groups.

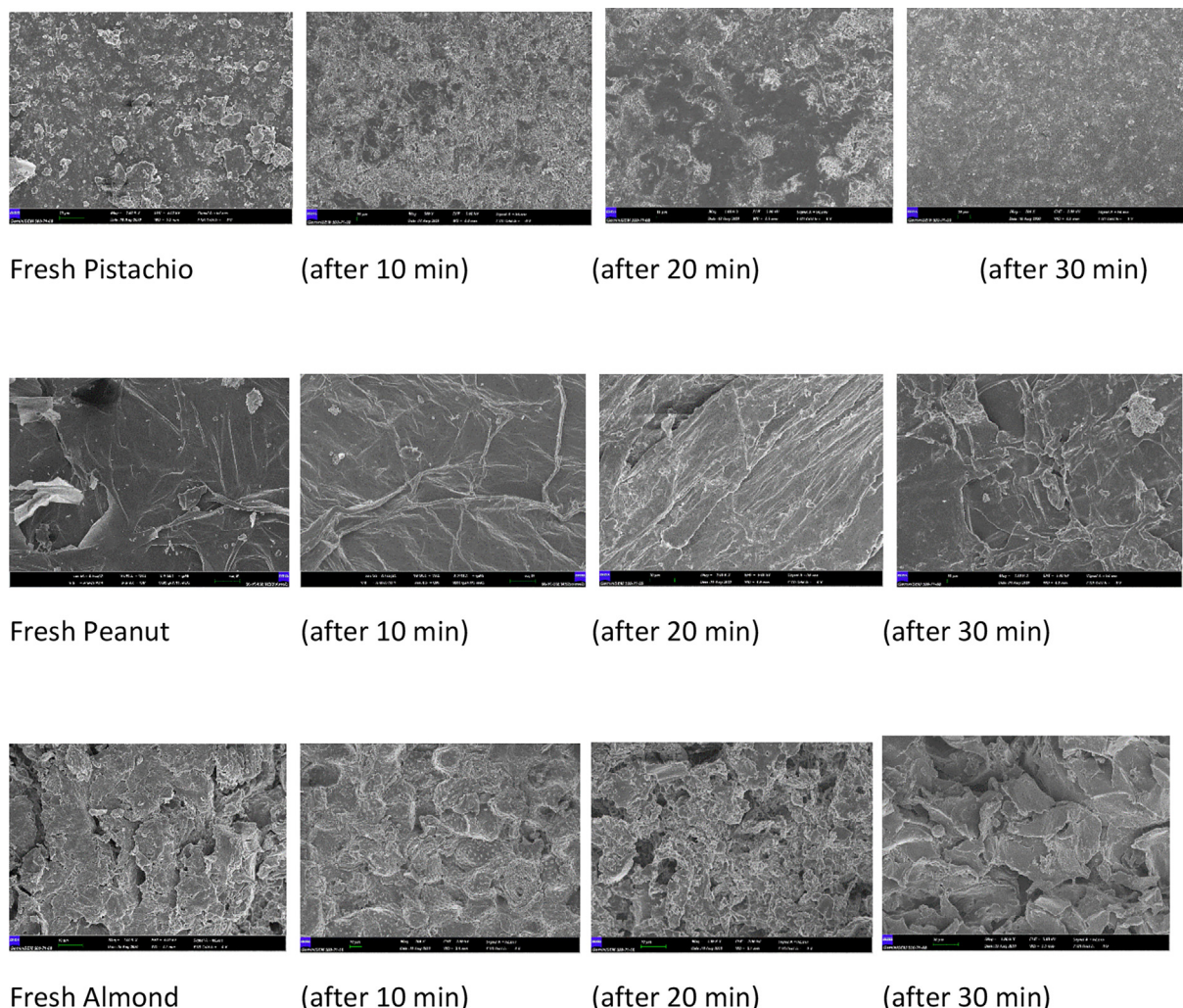


Fig. 2. SEM images of three adsorbent (Fresh, 10, 20 and 30 min).

2.5. Batch studies

Adsorbent, 1.0 g for three shells in a 100 mL-glass conical flask under initial Zn²⁺ concentration of 5, 10, 25, 50, and 100 mg/L, at an average 24 °C temperature, was used for the batch studies (in Erlenmeyer flasks), for 45 min of contact time. The flask was shaken by a d ZHICHENG analytical model thermal shaker at 150 rpm with pre-fixed time, ranged from 5 to 45 min. 2 mL supernatants for each including the initial solution were used at pre-fixed time intervals before the Zn²⁺ concentration determination. The amount of Zn²⁺ ions in solutions (qe) were calculated by using equations (1):

$$q_e = \frac{V(C_i - C_e)}{M} \tag{1}$$

where qe (mg g⁻¹) is the amount of metal ion removed from the solution, Ci (initial) and Ce (final) concentrations (mg/L), V is the volume (L) and M the mass of shells (g).

The studies were carried out in duplicate to ensure reproducibility, reliability, and accuracy of the data and the Origin 9.0 program (Origin Lab, USA) was also used for all data.

2.6. Error function analyses

In this study, the average relative error, normalized standard deviation and marquardt's percent standard deviation was also

applied experimental data to confirm the best fitting. The equations are given below;

$$ARE = \frac{100}{N} \sum_{i=1}^N \left| \frac{q_e^{exp} - q_e^{cal}}{q_e^{exp}} \right|_i \tag{2}$$

$$MPSD = 100 \sqrt{\frac{1}{N-p} \sum_{i=1}^N \left(\frac{q_{ei}^{exp} - q_{ei}^{cal}}{q_{ei}^{exp}} \right)^2} \tag{3}$$

$$NSD = 100 \sqrt{\frac{1}{N-1} \sum_{i=1}^N \left[\frac{q_t^{exp} - q_t^{cal}}{q_t^{exp}} \right]^2} \tag{4}$$

The MPSD, NSD and ARE shows more correct estimation of qe value (Kayranli, 2011).

3. Results and discussion

3.1. Characterization of adsorbents

The FTIR spectrums, scanned in the range of 450–4000 cm⁻¹, are demonstrated in Fig. 1. The spectra revealed many absorption peaks, indicating the complexity of the adsorbents. As seen in Fig. 1, the band at 3276 cm⁻¹ is indicating some hydroxyl groups (-OH) resulted from lignin, cellulose, hemicellulose in/on pistachio

shell. The band near 2843 and 2150 cm^{-1} is the stretching vibration of C–H in alkanes, aldehydes and a carboxylic acid, and $\text{C}\equiv\text{C}$ bond. The peak near 1722 cm^{-1} is the stretching vibration of C=O in aldehydes, and ketones. There is a complex set of absorptions unique to each compound in the fingerprint region (1500 cm^{-1} to 500 cm^{-1}) of the spectrum. It is described with the help of references instead of interpreting the peaks visually. The band around 1423 , 1251 , and 1148 cm^{-1} represents C=C alkanes, $-\text{NO}_2$ asymmetric nitro compound, and $-\text{CH}_3$, $-\text{CH}_2$ from alkanes, respectively. The peak 1026 cm^{-1} represents the C–O bond in cellulose. Peanut and almond shell also includes cellulose, hemicellulose and lining compounds, so similar spectra peaks came out as can be seen in Fig. 1. The adsorbent peak gives valuable information concerning the bond –OH groups, C=O stretching, secondary amino group, carbonyl/carboxyl group –C–C– functional group were mostly taken part in the adsorption process.

The SEM images of pistachio, peanut, and almond shell are also demonstrated in Fig. 2. It can be seen from the SEM images; shells consist of the number of heterogeneous pore layers.

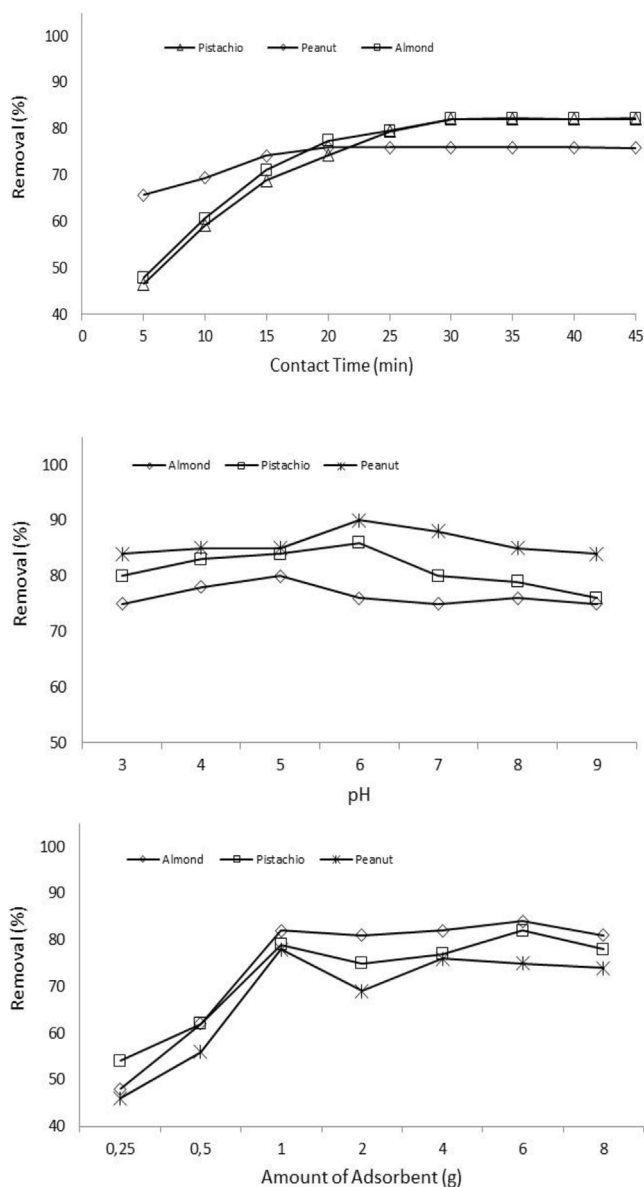


Fig. 3. Effect of contact time, pH and Adsorbent dosage on removal of zinc.

3.2. Contact time effect

Fig. 3 demonstrates the effect of time on Zn removal by shells. In the first 30 min, the removal rate increases quickly reaching a minimum of 83% for all adsorbents, and then increases in contact time have no critical effect on the rate and equilibrium was reached in about 45 min. Initial Zn^{2+} removal was rapid due to the large availability of functional groups on the adsorbent surface brought about the binding of metal ions on the adsorbent. The filling of functional groups on shells resulted in a decrease of Zn ions in the solution in the final stage (30–45 min) (see Fig. 3).

3.3. Effect of the pH

The adsorption capacity is, similarly, affected by pH due to the ability of hydrogen ions to change the adsorbent surface properties (Liu et al., 2017). Fig. 3 shows the effects of pH on the removal of Zn^{2+} . The removal efficiency of Zn^{2+} sharply changed for all adsorbents when the pH was increased from 3 to 6 and however, the removal rate fluctuated or decrease with an increased in pH values (pH = 9.0). The maximum removal rate was obtained at pH 6.0.

3.4. Effect of adsorbent dose

Adsorbent dose effect on the removal of metal ions is given in Fig. 3. The removal rate of Zn^{2+} increased significantly from 68% to 82% for Peanut due to the adsorbent dosage increase number of functional and active sites that resulted in removal efficiency. A similar trend is also valid for the pistachio and almond (see Fig. 3). The adsorbent dose increase from 0.25 to 8.0 g increases the removal efficiency first and then continues steadily. It can be explained by the relatively more existing reaction and binding sites in the surface area at lower adsorbent doses. The adsorbent dosage was selected as 1.0 g for the further batch experiments.

3.5. Adsorption isotherm

Freundlich (1906), Langmuir (1918), Temkin and Pyzhev (1940), Dubinin and Radushkevich (1947) isotherm models applied data obtained from the batch experiment, performed with altering initial Zn^{2+} concentrations ranging from 5 to 100 mg/L, to express the interactions. Isotherm linearized form of equations, parameters, and correlation coefficients is given in Table 1.

3.5.1. Freundlich isotherm;

The value of the Freundlich constant ($1/n$) informs the adsorption intensity and the sorption process is thought to be acceptable on the condition the value of n ranges between 1 and 10. As $1/n$ indicate that $1/n = 0$ is irreversible process, $0 < 1/n < 1$ is favourable adsorption and $1/n > 1$ unfavourable or cooperative adsorption. The value of $1/n$ for Zn^{2+} was calculated lower than unity and these were bigger than 0.99 for three adsorbent follows (see Table 1). It was concluded that the adsorption conditions were favourable, and an ion exchange process occurs in the uneven adsorption surface layer. The adsorption capacity of pistachio, peanut, and almond is as follows 17.28, 20.95, and 23.77 mg/g, respectively.

3.5.2. Langmuir isotherm;

The Langmuir constant (RL) gives information about the affinity of the sorbent for the binding ions. If $\text{RL} > 1$, the adsorption is undesirable; $\text{RL} = 1$, it is linear; $0 < \text{RL} < 1$ it is desirable; $\text{RL} = 0$, it is irreversible (Langmuir, 1918). Values of $1/n$ for adsorption on the shells were calculated as 0.912 for pistachio, 0.988 for peanut, and 0.943 for almond. These values confirmed that desirable adsorption occurs for the removal of metal ions by the organic adsorbents.

Table 1
Isotherm parameters for the adsorption of Zn²⁺.

Isotherms	Parameter					
		Correlation Coefficient	Pistachio	Peanut	Almond	
Freundlich $\log q_e = \log K_F + \frac{1}{n} \log C_e$	K _F		17.28	20.95	23.77	
	1/n		0.912	0.988	0.943	
	R ²		0.996	0.998	0.998	
	MPSD		8.13	8.41	4.39	
	NSD		6.30	2.01	3.69	
	ARE		4.83	2.0	2.31	
	Langmuir Type(I) $\frac{C_e}{q_e} = \frac{1}{q_{max}K_L} + \frac{C_e}{q_{max}} R_L = \frac{1}{1+C_0K_L}$	q _m		62.5	476.1	78.12
		KL		0.006	0.0007	0.0059
		RL		0.59	0.932	0.626
		R ²		0.60	0.86	0.48
MPSD			432.89	140.6	115.5	
NSD			335.31	108.9	89.4	
ARE			305	99.43	81.66	
Type(II) $\frac{1}{q_e} = \frac{1}{q_{max}K_L C_e} + \frac{1}{q_{max}}$		q _m		61.72	51.02	21.92
		KL		0.0065	0.069	0.022
		RL		0.603	0.589	0.310
	R ²		0.987	0.989	0.978	
	MPSD		15.08	16.59	21.04	
	NSD		23.94	25.11	18.55	
	ARE		8.66	9.07	4.26	
	Temkin $q_e = \frac{RT}{A_1} \ln K_T + \frac{RT}{A_1} \ln C_e$	q _m		2.3117	2.3327	2.3322
		KT		0.745	0.6468	0.8326
		R ²		0.8551	0.8461	0.8392
MPSD			167.95	182.35	173.42	
NSD			130.10	141.2	134.33	
ARE			72.30	78.70	75.81	
Dubinin–Radushkevich $\ln q_e = \ln q_m - \beta \varepsilon^2$		q _m		3.243	3.059	3.2576
		β		0.008	0.0093	0.0066
		ε		7.90	7.33	8.70
		R ²		0.7065	0.6837	0.5913
	MPSD		77.63	57.86	55.95	
	NSD		60.13	50.115	48.45	
	ARE		49.72	34.69	33.76	

Fig. 4 presents the comparison of the experimental values, and the predicted amount of equilibrium for pistachio, peanut and almond shell. As demonstrated in Fig. 4, the data calculated values by Langmuir isotherm are close to the experimental data and the best isotherm for predicting the amount of Zn²⁺ adsorbed on the shells at equilibrium. Furthermore, the values of ARE, NSD, and MPSD error analysis are well fit to Langmuir isotherms provides a better model for the reduction of Zn²⁺ (see Table 1). The correlation coefficient (R²), however, shown that Temkin and Dubinin–Radushkevich models application for three adsorbents in this study is limited.

3.6. Kinetic studies

To analyse the adsorption process, diffusion rate and mechanism of Zn²⁺ the Elovich (Kayranli, 2011), Lagergren pseudo-first-order (Lagergren, 1898), and the pseudo-second order model (Ho and McKay, 2003), and the intra-particle diffusion model (Weber and Morris, 1963) were applied, and the linearized equations are given in Table 2. The coefficients (R²) of Zn²⁺ on the shells were calculated >0.99 for pseudo-second order. So, the pseudo-second order is well described in comparison to the pseudo first order in the adsorption process of Zn²⁺. Previous researchers (Lee and Choi, 2018) pointed out that pseudo-second order is more applicable than pseudo-first order to analyse the sorption rate of most sorbents in the aqueous medium. Similar results were found to remove Zn²⁺ by using shells and our results are in line with previous studies.

As seen in Fig. 5, the intra-particle diffusion plot can separate a few linear regions, and the results demonstrated that not only intra-particle diffusion is the rate-limiting mechanism in the process, but also diffusion played an important role. The adsorption

process was governed by more than one mechanism such as external mass transfer and internal particle diffusion.

3.7. Removal mechanism of zinc

Heavy metals and functional groups interaction is complex and affected by adsorbent properties, porous structure, surface area, and functional groups, pH of the solution, metals chemistry in solution, binding characteristics that affects adsorption behaviours. The heavy metals adsorption process is mostly carried out by mechanism of ion exchange, electrostatic interaction, complex formation, surface complexation, physical adsorption, and/or precipitation (Kaur et al., 2020). Each mechanism specific role depends on functional groups of organic adsorbent, ionization of metals, and aqueous environment (Neris et al., 2019a). The main constituents of the three used organic residuals are lignin, cellulose, and hemicellulose, and also other components are, lipids, proteins, simple sugars, and ash, having a different ratio. Cellulose consists of 49.39% oxygen, 44.44% carbon, and 6.17% hydrogen with having a linear chain. There are many active sites on/in the shells, such as –COOH, –OH, –CH₃, –NO₂, –CH₂, –CH, amino acids, and so on, involving in the heavy metal removal process.

FTIR spectra of the shell at 10-minute intervals during Zn²⁺ adsorption showed that functional groups of hydroxyl, carbonyl/carboxyl play important roles in the adsorption of heavy metals, and zinc adsorption by the shells increased over time. This adsorption resulted in changing the peaks and transmittances (see Table 3).

The spectroscopic analysis of the pistachio shell during the removal process demonstrated the peak transmittance shifted from 87.0 to 80.0 % (3276 cm⁻¹) for hydroxyl groups, and 94.0 to 87.0% for the peak of 2056 cm⁻¹ of alkanes, aldehydes, and car-

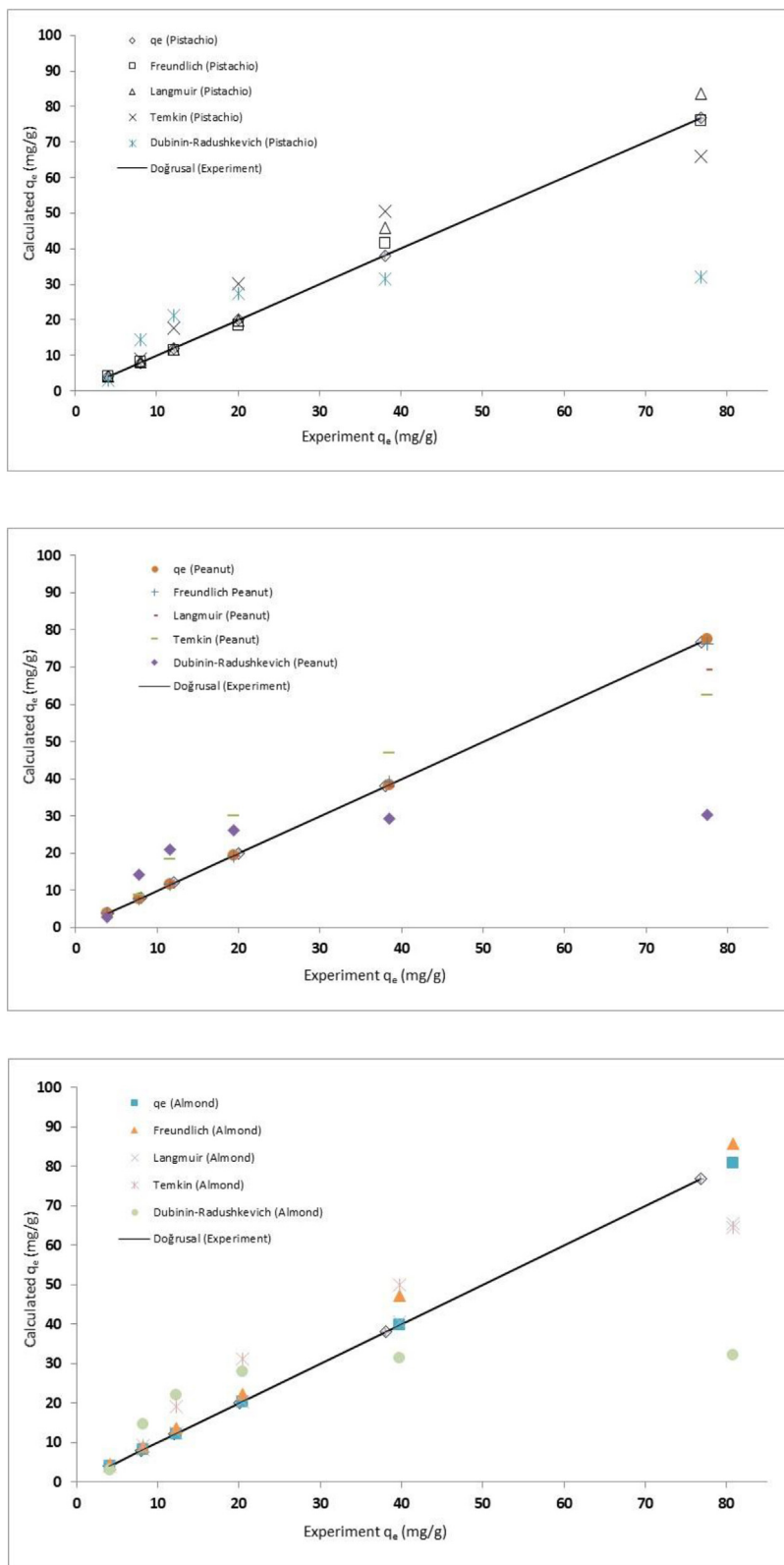


Fig. 4. The predicted amount of adsorbents at equilibrium by different isotherm models and the experimental values.

boxylic groups (C–H); 1722 cm^{-1} assigned for aromatic C–C transmittance decrease 6.0%; 1148 cm^{-1} assigned for C=O ester and carboxyl groups transmittance altered from 93.0 to 87.5%. The band at 3331 cm^{-1} is indicating a number amount of hydroxyl (–OH) groups is produced from lignin, cellulose, hemicellulose,

the transmittance decreased 11.0% for the almond shell. The peak near 2918 cm^{-1} is the stretching vibration of C–H in alkanes, aldehydes and carboxylic acid, and changed to 16.5% end of the process. Furthermore, the peak at 3272 cm^{-1} refers to the hydroxyl groups (–OH) transmittance changed from 84.0 to 79% (30 min) for

Table 2
Kinetic parameters for the adsorption of Zn²⁺.

Kinetic Model	Parameters				
	Coefficient	Constant	Pistachio	Peanut	Almond
Elovich $q_t = \frac{1}{\beta} \ln(\alpha\beta) + \frac{1}{\beta} \ln t$	β		0.3142	0.0225	0.2964
	α		4.5977	1.2878	1.5344
	R^2		0.893	0.902	0.7802
	MPSD		54.16	56.42	58.06
	NSD		15.20	238.99	50.28
	ARE		12.27	46.05	47.36
Pseudo-first order $\ln(q_e - q_t) = \ln q_e - k_1 t$	q_e		0.8858	6.240	1.267
	k_{1p}		0.0039	0.0241	0.0937
	R^2		0.57	0.411	0.402
	MPSD		98.67	185.97	59.03
	NSD		85.45	161.05	279.70
	ARE		65.78	321.14	39.04
Pseudo-second order $\frac{t}{q_t} = \frac{1}{k_2 q_e^2} + \frac{t}{q_e}$	q_{me}		8.5324	4.2194	4.3
	K_{2p}		0.2980	0.3390	0.2756
	R^2		0.9999	0.9999	0.9996
	MPSD		1.42	128.89	2.21
	NSD		82.60	0.9445	1.91
	ARE		26.12	0.0326	0.032
Intra-particle Diffusion $q_t = k_p \sqrt{t} + C$	k_p		3.4117	1.4291	1.667
	R^2		0.890	0.4987	0.3247
	MPSD		153.66	31.29	31.89
	NSD		133.08	27.09	27.61
	ARE		115.96	20.85	22.81

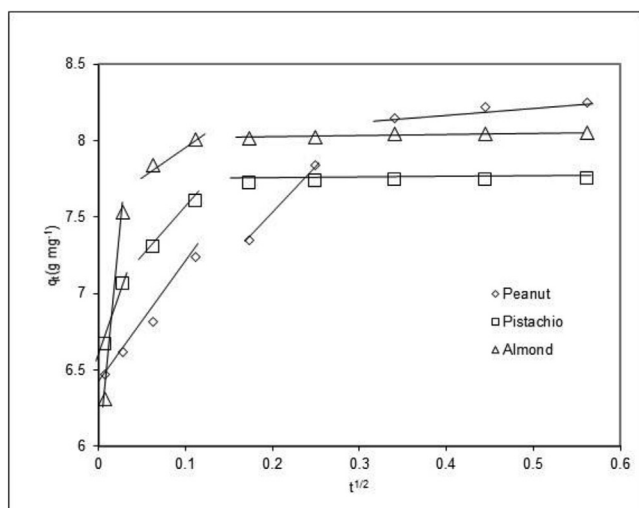


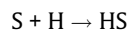
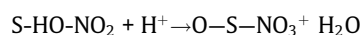
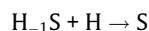
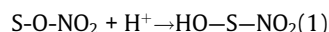
Fig. 5. Intra-particle diffusion plots of the pistachio, peanut, and almond for zinc.

the peanut shell. It is most likely that surface adsorption through their complexation with the phenolic -OH group occurs. The bands at 1728–1606 cm⁻¹ for peanut were linked with the aromatic carbonyl/carboxyl C=O and the aromatic C=C stretching modes, and changes of these peaks after adsorption started surface complexation of Zn²⁺ by delocalized electrons. The peak near 1728 of transmittance changed 9.0% (30 min), is the vibration of C=O in aldehydes and ketones for almond. Similarly, the peaks at around 1597 and 1504 cm⁻¹ were assigned to C-O vibrations of hydroxyl groups or C-H stretching vibrations resulted from cellulose, hemicellulose and lignin and that of transmittance shifted 11.5% and 16.5 %, respectively. As seen in Table 3, the transmittance shifts informed that the bond -OH groups, C=O stretching, secondary amino group, carboxyl group -C- functional group were mostly taken part in the adsorption process. The -OH and -COOH groups were involved in the adsorption process due to C=O and -OH functional groups changed after zinc adsorption. These changes could be explained by the ion-exchange mechanism between adsorbent and adsorbate. The actives groups can cooperate with ions in many

ways, as shown in Fig. 6. it can be concluded that the electrostatic interaction, ion exchange, diffusion, formation of complex, and Zn ions sorption by surface functional groups are the mechanism of the metal ions removal process.

3.8. Electrostatic interaction

The electrostatic interaction is created as a result of divalent metals and negatively charged functional groups on the adsorbent. However, this happens secondary and is very weak. The aqueous pH, and point of zero charges of the adsorbent are key for the frequency of electrostatic interaction (Yang et al., 2019). Therefore, the carboxyl groups were dissociated and associated with the Zn²⁺ ions due to the working pH value is 6.0. Three adsorbent shell is represented by S, and the protonation equilibria for the nitro, -NO₂ and the hydroxyl of C-6, -OH is as follows;

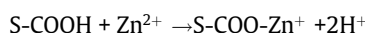
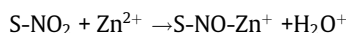
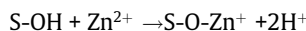
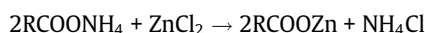
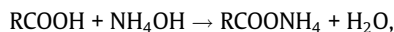


3.9. Ion-exchange

The other main heavy metal removal process is that ion exchange takes place with the availability of carboxyl and hydroxyl functional groups include oxygen. The functional group chemistry and metal ion size are critical for process efficiency (Yang et al., 2019). Specifically, an acidic functional group plays a critical role in the removal of heavy metals by organic adsorbents. The zinc removal rate increased at pH 6.0 due to negatively adsorption surface increased. pH was adjusted by using NH₄OH in this study, resulting in hydroxide to form the Zn(HO)₂ salt. Based on the results, one of the adsorption mechanisms is cation exchange due to removal efficiency affected by pH (Ali et al., 2016). The ion exchange process is most likely defined by the following equations:

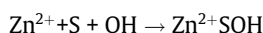
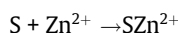
Table 3
Adsorbents functional groups and transmittance change in the process.

R Peak	Pistachio Transmittance %			Peanut Transmittance %			Almond Transmittance %			Assignment
	Before ads.		Peak	Before ads.		Peak	Before ads.		Peak	
	(10 min)	(20 min)	(30 min)	(10 min)	(20 min)	(30 min)	(10 min)	(20 min)	(30 min)	
3276	87.0	76.0	3272	84.0	76.0	79.0	3331	97.0	86.0	-OH (hydroxyl, carboxyl acid groups)
2056	94.0	85.0	2893	86.0	77.0	81.0	2918	98.5	82.0	C-H (aliphatic structures, alkane), symmetric, asymmetric -CH ₂ groups, C≡
1722	88.0	76.0	1728	94.0	-	86.0	1728	98.5	89.5	C=O (ester, carboxyl groups)
1597	92.0	83.0	1606	85.0	74.0	82.0	1597	98.0	89.5	C-O, C=O (ester, carbonyl, carboxyl groups and aromatic rings)
1504	96.0	87.0	1507	90.0	86.0	88.0	1504	99.5	83.0	C=C (aromatic rings)
1413	86.0	80.0	1423	87.5	85.5	86.0	1416	99.0	83.5	C-C, CO ₃ (carbonate)
1229	86.0	77.0	1251	88.0	78.0	85.0	1226	98.0	88.0	C=O, OH, S=O
1148	93.0	84.0	1148	90.0	86.0	85.0	1148	95.0	84.0	C=O (ester, carboxyl groups)
1026	82.0	67.0	1018	81.0	72.0	72.0	1011	96.0	85.0	C=O (ester, carboxyl groups)



3.10. Surface complexations

Surface complexations occur with multi atom structures and metal-functional group interaction and important processes in adsorption. The carboxyl/carbonyl functional groups bind heavy metals, creating a complexation (Neris et al., 2019b). (Ali et al., 2016) pointed out that chemical adsorption may be the rate controlling step due to forming chemical bonds with exchange or sharing of electrons between sorbent and sorbate in process. The complex species associated with equilibrium can be defined by the following equations;



3.11. Diffusion

Fernández-López et al. (Fernández-López et al., 2019) pointed out that some information relating to the adsorbent surface, chemical/physical reaction, and diffusion, the relevant proper reaction rate is described by the sorption kinetic models. The adsorption-complexation interactions through electron exchange or sharing are the main sorption processes.

Therefore, an intra-particle diffusion model was applied to define the adsorption kinetics due to the porous structure of the shells. The first plot refers to the external surface adsorption in the intra-particle diffusion model. The first stage is the fastest adsorption process due to the presents of unbinding sites. The second part, the gradual adsorption stage, is defined with intra-particle diffusion of the metal ions through the pores of shell particles. The final equilibrium stage represents the intra-particle or both film and intra-particle diffusion due to the low metal ions remain in the solution. During the adsorption of Zn²⁺ onto the shells, sequencing steps take place and are represented in Fig. 6.

3.12. Use of end-product as a soil conditioner

Cultivation trends, currently, focus on using bio-organic fertilizer/conditioner instead of chemical fertilizers due to high costs, contamination, and inappropriate application causing soil quality degradation (Omoni et al., 2020). The world trend is to protect soil biodiversity while producing quality crops for sustainability. Organic fertilizers, produced organic wastes, are cheap nutrient sources and enhance crop production in low-input agriculture. Furthermore, organic waste increases soil organic carbon and microbial activity that helps provides nutrients and recycling them for plant growth (Hafez et al., 2021).

Zinc is an essential micronutrient and affects most of the physiological processes (Broadley et al., 2007). The presence of major nutrients concentrations and the microelements forms for plant usage is affected by soil pH, affecting also total Zn concentration

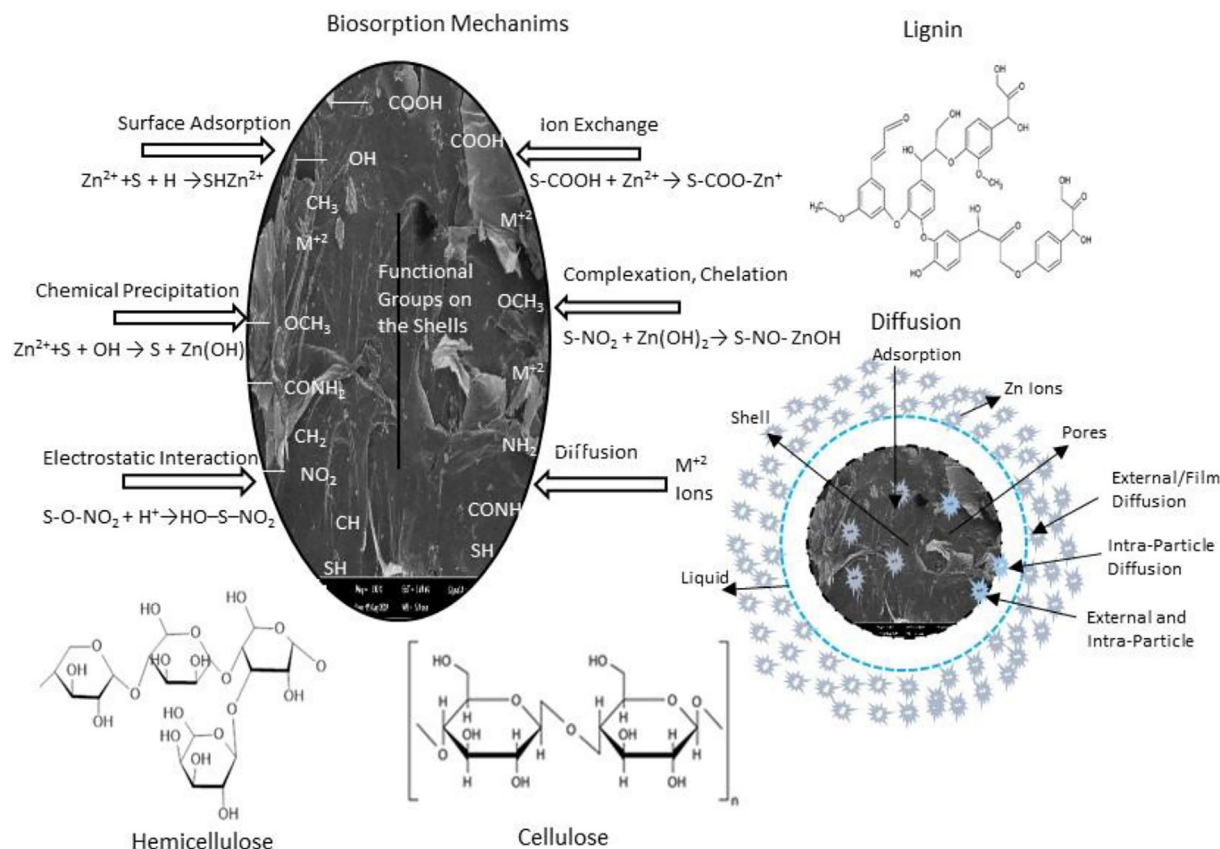


Fig. 6. Possible adsorption mechanisms of Zn^{2+} .

and activity in soil solution, and high pH removes the total Zn concentration and activity (Bonten et al., 2008). Calcareous soil lacks nutrients, especially N, P, micro-nutrients, and soil organic matter, resulted in weak soil–plant productivity. Bio-organic conditioners decrease nutrient losses and enhance plant growth in calcareous soil (Hafez et al., 2021). Fresh shells contain organic materials, nutrients and mineral and then holding zinc with functional groups make it valuable soil conditioner/ amendments. The ideal soil pH for plant growth is between 6.0 and 8.0 called neutral soil. The end-product can also be used for reducing the pH of the alkaline and high alkaline soil ($pH > 8$).

4. Conclusions

This study has shown that pistachio, peanut, and almond shell can be used for reducing Zn^{2+} from aqueous solutions as an eco-friendly, low-cost adsorbent. The maximum adsorption capacity of pistachio, peanut, and almond is as follows; 59.52 mgg^{-1} , 54.64 mgg^{-1} , and 51.81 mgg^{-1} , respectively. Adsorption ability of the adsorbent for Zn^{2+} uptake was as followed: Pistachio > Peanut > Almond. Functional groups on shell surfaces can cooperate with metal ions in many ways, electrostatic interaction, diffusion, ion exchange. Furthermore, the by-product containing organic compounds and zinc can be used as a soil conditioner for agriculture, resulting in decreasing the disposal cost of the by-products for sustainable environmental management.

Declaration of Competing Interest

The authors declare that they have no known competing financial interests or personal relationships that could have appeared to influence the work reported in this paper.

References

- Ali, I., Alharbi, O.M.L., Allothman, Z.A., Alwarthan, A., 2018a. Facile and eco-friendly synthesis of functionalized iron nanoparticles for cyanazine removal in water. *Colloids Surfaces B Biointerfaces* 171, 606–613. <https://doi.org/10.1016/j.colsurfb.2018.07.071>.
- Ali, I., Alharbi, O.M.L., Tkachev, A., Galunin, E., Burakov, A., Grachev, V.A., 2018b. Water treatment by new-generation graphene materials: hope for bright future. *Environ. Sci. Pollut. Res.* 25 (8), 7315–7329. <https://doi.org/10.1007/s11356-018-1315-9>.
- Ali, I., Babkin, A.V., Burakova, I.V., Burakov, A.E., Neskromnaya, E.A., Tkachev, A.G., Panglisch, S., AlMasoud, N., Alomar, T.S., 2021a. Fast removal of samarium ions in water on highly efficient nanocomposite based graphene oxide modified with polyhydroquinone: Isotherms, kinetics, thermodynamics and desorption. *J. Mol. Liq.* 329, 115584. <https://doi.org/10.1016/j.molliq.2021.115584>.
- Ali, I., Gupta, V.K., Aboul-Enein, H.Y., 2005. Metal ion speciation and capillary electrophoresis: Application in the new millennium. *Electrophoresis* 26, 3988–4002. <https://doi.org/10.1002/elps.200500216>.
- Ali, I., Kon'kova, T., Kasianov, V., Rysev, A., Panglisch, S., Mbianda, X.Y., Habila, M.A., AlMasoud, N., 2021b. Preparation and characterization of nano-structured modified montmorillonite for dioxidine antibacterial drug removal in water. *J. Mol. Liq.* 331, 115770. <https://doi.org/10.1016/j.molliq.2021.115770>.
- Ali, R.M., Hamad, H.A., Hussein, M.M., Malash, G.F., 2016. Potential of using green adsorbent of heavy metal removal from aqueous solutions: Adsorption kinetics, isotherm, thermodynamic, mechanism and economic analysis. *Ecol. Eng.* 91, 317–332. <https://doi.org/10.1016/j.ecoleng.2016.03.015>.
- Basheer, A.A., 2018. New generation nano-adsorbents for the removal of emerging contaminants in water. *J. Mol. Liq.* 261, 583–593. <https://doi.org/10.1016/j.molliq.2018.04.021>.
- Bonten, L.T.C., Groenenberg, J.E., Weng, L., van Riemsdijk, W.H., 2008. Use of speciation and complexation models to estimate heavy metal sorption in soils. *Geoderma* 146 (1–2), 303–310. <https://doi.org/10.1016/j.geoderma.2008.06.005>.
- Broadley, M.R., White, P.J., Hammond, J.P., Zelko, I., Lux, A., 2007. Zinc in plants. *New Phytol.* 173 (4), 677–702. <https://doi.org/10.1111/j.1469-8137.2007.01996.x>.
- Dubinina, M.M., Radushkevich, L.V., 1947. The Equation of the Characteristic Curve of Activated Charcoal. *Proc. Acad. Sci. Phys. Chem. Sect.* 55, 331–337.
- FAO, 2020. FAOSTAT. <http://www.fao.org/faostat/en/#data/QL>, n.d.
- Fernández-López, J.A., Angosto, J.M., Roca, M.J., Doval Miñarro, M., 2019. Taguchi design-based enhancement of heavy metals bioremoval by agroindustrial waste biomass from artichoke. *Sci. Total Environ.* 653, 55–63. <https://doi.org/10.1016/j.scitotenv.2018.10.343>.

- Freundlich, H.M.F., 1906. Over the Adsorption in Solution. *J. Phys. Chem.* 57, 385–471.
- Hafez, M., Popov, A.I., Rashad, M., 2021. Environmental Technology & Innovation Integrated use of bio-organic fertilizers for enhancing soil fertility – plant nutrition, germination status and initial growth of corn (*Zea Mays L.*). *Environ. Technol. Innov.* 21, <https://doi.org/10.1016/j.eti.2020.101329> 101329.
- Hamad, H.T., 2021. Removal of phenol and inorganic metals from wastewater using activated ceramic. *J. King Saud Univ. - Eng. Sci.* 33 (4), 221–226. <https://doi.org/10.1016/j.jksues.2020.04.006>.
- Ho, Y.S., McKay, G., 2003. Sorption of dyes and copper ions onto biosorbents. *Process Biochem.* 38 (7), 1047–1061. [https://doi.org/10.1016/S0032-9592\(02\)00239-X](https://doi.org/10.1016/S0032-9592(02)00239-X).
- Langmuir, I., 1918. Adsorption of gases on plain surfaces of glass, mica and platinum. *J. Am. Chem. Soc.* 40, 1361–1403.
- Kaur, M., Kumari, S., Sharma, P., 2020. Removal of Pb (II) from aqueous solution using nanoadsorbent of *Oryza sativa* husk: Isotherm, kinetic and thermodynamic studies. *Biotechnol. Reports* 25, e00410. <https://doi.org/10.1016/j.btre.2019.e00410>.
- Kayranli, B., 2011. Adsorption of textile dyes onto iron based waterworks sludge from aqueous solution; isotherm, kinetic and thermodynamic study. *Chem. Eng. J.* 173 (3), 782–791. <https://doi.org/10.1016/j.cej.2011.08.051>.
- Lagergren, S., 1898. About the theory of so-called adsorption of soluble substances. *Kungliga Svenska Vetenskapsakademiens Handlingar*.
- Lee, S.Y., Choi, H.J., 2018. Persimmon leaf bio-waste for adsorptive removal of heavy metals from aqueous solution. *J. Environ. Manage.* 209, 382–392. <https://doi.org/10.1016/j.jenvman.2017.12.080>.
- Liu, X., Lu, S., Liu, Y., Meng, W., Zheng, B., 2017. Adsorption of sulfamethoxazole (SMZ) and ciprofloxacin (CIP) by humic acid (HA): Characteristics and mechanism. *RSC Adv.* 7 (80), 50449–50458. <https://doi.org/10.1039/C7RA06231A>.
- Lonergan, Z.R., Skaar, E.P., 2019. Nutrient Zinc at the Host-Pathogen Interface. *Trends Biochem. Sci.* 44 (12), 1041–1056. <https://doi.org/10.1016/j.tibs.2019.06.010>.
- Temkin, M.J., Pyzhev, V., 1940. Recent modifications to langmuir isotherms. *Acta Physicochim* 12, 217–222.
- Mu'azu, N.D., Essa, M.H., Lukman, S., 2019. Scale-up of hybrid electrokinetic-adsorption technique for removal of heavy metals from contaminated saline-sodic clay soil. *J. King Saud Univ. - Eng. Sci.* 31 (2), 122–130. <https://doi.org/10.1016/j.jksues.2016.12.002>.
- Neris, J.B., Luzardo, F.H.M., da Silva, E.G.P., Velasco, F.G., 2019a. Evaluation of adsorption processes of metal ions in multi-element aqueous systems by lignocellulosic adsorbents applying different isotherms: A critical review. *Chem. Eng. J.* 357, 404–420. <https://doi.org/10.1016/j.cej.2018.09.125>.
- Neris, J.B., Luzardo, F.H.M., Santos, P.F., de Almeida, O.N., Velasco, F.G., 2019b. Evaluation of single and tri-element adsorption of Pb²⁺, Ni²⁺ and Zn²⁺ ions in aqueous solution on modified water hyacinth (*Eichhornia crassipes*) fibers. *J. Environ. Chem. Eng.* 7 (1), 102885. <https://doi.org/10.1016/j.jece.2019.102885>.
- Oliveira, D.A., Benelli, P., Amante, E.R., 2013. A literature review on adding value to solid residues: Egg shells. *J. Clean. Prod.* 46, 42–47. <https://doi.org/10.1016/j.jclepro.2012.09.045>.
- Omoni, V.T., Lag-Brotons, A.J., Semple, K.T., 2020. Impact of organic amendments on the development of 14C-phenanthrene catabolism in soil. *Int. Biodeterior. Biodegrad.* 151, 104991. <https://doi.org/10.1016/j.ibiod.2020.104991>.
- Wang, R., Yan, Q., Su, P., Shu, J., Chen, M., Xiao, Z., Han, Y., Cheng, Z., 2020. Metal mobility and toxicity of zinc hydrometallurgical residues. *Process Saf. Environ. Prot.* 144, 366–371. <https://doi.org/10.1016/j.psep.2020.07.042>.
- Weber, W.J., Morris, J.C., 1963. Kinetics of Adsorption on Carbon from Solution. *J. Sanit. Eng. Div.* 89 (2), 31–59.
- Yang, X., Wan, Y., Zheng, Y., He, F., Yu, Z., Huang, J., Wang, H., Ok, Y.S., Jiang, Y., Gao, B., 2019. Surface functional groups of carbon-based adsorbents and their roles in the removal of heavy metals from aqueous solutions: A critical review. *Chem. Eng. J.* 366, 608–621. <https://doi.org/10.1016/j.cej.2019.02.119>.